The Early Paleogene: A Glimpse of an Extremely Warm World

Jacob Slawson (jslawson@mines.edu)
Colorado School of Mines https://orcid.org/0000-0002-3427-163X
Piret Plink-Björklund
Colorado School of Mines https://orcid.org/0000-0003-1637-2100
Thomas Reichler
University of Utah https://orcid.org/0000-0002-5004-0110
Daniel Baldassare
University of Utah

Physical Sciences - Article

Keywords:

Posted Date: November 14th, 2023

DOI: https://doi.org/10.21203/rs.3.rs-3428515/v1

Additional Declarations: There is **NO** Competing Interest.

Abstract

As the world warms, the Earth system moves towards a climate state without societal precedent[1]. This challenges predictions of the future, as climate models need to be tested and calibrated with real-world data from high carbon dioxide climates[2]. Despite the many advances in climate modeling, predictions of precipitation have particularly high uncertainties[3]. Earth history provides an opportunity to observe how the Earth system responded to high greenhouse gas emissions, enabling us to better predict how it may do so in the future. Here, we compile global proxy data from the Early Paleogene (66 – 49 Ma), a period with a warm climate overprinted by multiple rapid global warming events[4], and suggested as a possible analogue for future worst-case scenarios[1, 2]. We show surprising results in the timing and duration of dramatic shifts in the hydrologic cycle occurring well prior to maximum temperatures and persisting well beyond. We provide a glimpse of an extremely warm Earth with ever-wet or monsoonal conditions in the northern and southern polar regions, and sustained aridity interrupted by extreme rainfall events at mid-latitudes. Our results indicate inconsistencies between proxy data and state-of-the-art paleoclimate models that are commonly used to predict and understand future climate change. Our focus on precipitation intermittency and intensity provides new data on long-term precipitation trends in high greenhouse gas climates to help address large uncertainties in future precipitation trends.

Main Text

Despite the significant threats that climate change poses to our society and ecosystems, future changes related to precipitation, and thus water availability, droughts, and floods are not well understood[5]. A strategy for assessing the effects of greenhouse gas forcing on climate is to turn to Earth's past where changes in climate and the Earth system are stored in the form of sedimentological, paleontological, isotopic, and geochemical proxies[3]. The Late Paleocene and Early Eocene epochs of the Early Paleogene period are composed of a series of rapid global warming events referred to as hyperthermals[4]. These events were orbitally paced and likely driven by large-scale releases of isotopically light carbon to the ocean-atmosphere system[6, 7]. These hyperthermals are documented in both the marine and terrestrial sedimentary records as negative carbon isotope excursions, deep-sea carbonate dissolution, and ecosystem disruptions[4, 8, 9]. Although greenhouse gas emission rates are higher today[10], the Early Paleogene offers a remarkable opportunity to study changes in climate in response to extreme greenhouse gas forcing because temperatures and carbon dioxide concentrations were similar to the worst-case-scenario greenhouse gas emission predictions[1, 2]. Furthermore, the paleogeography is reasonably well constrained with a similar continental configuration to that of today[11].

The largest carbon release of the Early Paleogene occurred during the Paleocene-Eocene Thermal Maximum (PETM), the warmest period of the Cenozoic Era (~ 14°C warmer than the 1961–1990 mean), lasting from 55.9–55.7 million years ago (Ma)[12]. The PETM was preceded by a warming trend and hyperthermals during the Late Paleocene beginning at approximately 59 Ma, and it was followed by a series of hyperthermals from approximately 53 to 49 Ma, a period known as the Early Eocene Climatic

Optimum (EECO)[13]. While changes in mean temperature conditions during the PETM and EECO have been reconstructed at a relatively high resolution at the poles and mid-latitude locations[14], changes in precipitation are not well understood[15]. Modeling studies of the PETM indicate that rather than a “wet gets wetter, dry gets drier" alteration of climate[16], there was an increase in extreme precipitation events with complex regional responses, such as increased mid-latitude atmospheric rivers and decoupling of mean annual precipitation from precipitation intermittency and intensity[17, 15].

Much prior research has focused on the PETM[12, 15], and on mean climate conditions during the Early Paleogene at discrete locations[8, 18]. A global understanding of climate during the Early Paleogene is needed to better understand the Earth system’s response to rapid global warming events and compare to climate model outputs. Here, we compile proxy data on a global scale over a longer time period (66 – 49 Ma) comprised of multiple global warming events and synthesize the data in a novel way to create the first climate maps for the Early Paleogene. We present these data as interactive maps where data and their uncertainties are presented in a transparent way (SI Data S2 and S3). By looking at conditions preceding and following hyperthermals, we investigate how the Earth system responded spatially and temporally to extreme greenhouse gas forcing in the past. We address global trends and focus on precipitation extremes and intermittency to help address large uncertainties in future precipitation trends[15, 19]. We find large and unusual shifts in climate that have not been documented previously and are surprising in terms of their timing and duration. Furthermore, we address inconsistencies between this proxy compilation and paleoclimate models that are commonly used to more accurately predict and understand future climate changes[2].

Deciphering Past Climates

Climate proxies are not direct indicators for changes in climate but rather provide indirect evidence for how temperature and hydrological changes impacted the Earth surface or biota in the geological past[5, 12]. As such, proxies are most convincing when used as multi-proxy investigation, but even then they may prove to be ambiguous for interpretations or comparison with modern instrumental data[20]. It follows that large uncertainties are associated with paleoclimate analyses. For example, the climate at discrete locations may not be representative of regional climate, especially due to topographic effects. To overcome these ambiguities, we use multi-proxy analyses wherever possible and synthesize the proxy data into broad climate types with distinct ranges of mean annual surface temperature (MAT), mean annual precipitation (MAP) and precipitation seasonality, intermittency and intensity (Table 1; see also SI “Climate type definitions”). This climate classification system broadly follows the Whittaker vegetation plots[21], the Köppen-Geiger climate classification[22], and the paleo-Köppen-Geiger system[23] but with a novel focus on precipitation intermittency and intensity. We then track how climate changed through the Paleogene hyperthermals for comparison to the modern world (Fig. 1).

Table 1
Climate type definitions.

Climate	Mean Annual Temperature	Mean Annual Precipitation	Modern Example
Warm, ever-wet (WEW) or cool, ever-wet (CEW)	WEW: >20°C CEW: <20°C	Perennial, ever-wet > 2000 mm/yr	WEW: Amazon rainforest CEW: Western Washington, USA
Warm Monsoonal (WM) or cool monsoonal (CM)	WM: >20°C CM: <20°	Seasonal monsoonal, 500–2000 mm/yr	M: India CM: Japan
Sub-humid (WS) or semi-arid (CS)	WS: >20°C CS: <20°C	WS: Intermittent, 500–2000 mm/yr CS: Intermittent, < 500–1200 mm/yr	WS: Cameroon CS: Colorado, USA
Warm (WA) or cool arid (CA)	WA: >20°C CA: <20°C	Intermittent, < 500 mm/yr	WA: Algeria CA: Southern Kazakhstan
Humid subtropical (HS) or cool temperate (CT)	HS: >15°C CT: <15°C	Perennial, 500–2000 mm/yr	HS: Florida, USA CT: Poland
Cold, dry with seasonal freeze-thaw (CD)	-5 to 5°C	Perennial, 500–1500 mm/yr	Yukon, Canada

We utilize and build upon recent progress made in developing new ways to assess climate proxy reliability and uncertainty[14]. The proxy data is both qualitative and quantitative and includes leaf fossil analyses, ancient soil geochemistry, river sedimentology, and clay mineralogy (SI “Climate proxies”). Where data was qualitative, a range of mean annual precipitation and precipitation intermittency values were inferred based on comparison to modern analogues (SI “Climate type definitions”). The proxy data was binned into the six time periods to enable us to investigate climate prior to, during, and after the Early Paleogene hyperthermals: Early Paleocene (66 – 59 Ma), Late Paleocene (59-55.9 Ma), PETM (55.9–55.7 Ma), Post-PETM (55.7–53 Ma), EECO (53 – 49 Ma), and Post-EECO (< 49 – 47 Ma).

Modern Climate

Our climate classification system can be applied to both the modern and Early Paleogene world (Fig. 1). The modern world (Fig. 1A) has polar ice caps and cold, dry conditions at high latitudes. Mid-latitudes are temperate with perennial precipitation. Semi-arid or sub-humid conditions are also common at mid-latitudes that are continental and/or located on the leeside of mountain ranges. Large arid, subtropical regions are located around 30° latitude and characterized by high pressure, dry climate, and major deserts related to the descending Hadley Cell and ocean circulation[24]. Near the equator, precipitation is part of the

rising Hadley Cell and the seasonally migrating inter-tropical convergence zone[25]. Here, the climate is either warm monsoonal or warm, ever-wet and MAP is generally greater than 2000 mm/yr.

Early Paleogene Climate

Climate during the Early Paleocene (Fig. 1B) was similar to the modern world with the exception of high latitudes that were considerably warmer, wetter, and ice-free. Northern high latitudes had a cool, ever-wet climate (CEW), while southern high latitudes were cool monsoonal (CM). This drastic difference from the modern world may indicate altered ocean or atmosphere circulation at high latitudes beginning in the Early Paleocene. Similar to the modern world, mid-latitudes (30–60°) were temperate (CT), or characterized by cool to warm temperatures and perennial precipitation, with some sub-humid or semi-arid locations (WS/CS) at continental interiors. A few proxy locations in the western United States are indicative of warm monsoonal conditions (WM), suggesting that the southwestern United States was wetter than today, despite a similar latitudinal position to the present. Similarly, subtropical North Africa was humid subtropical (HS) with a climate similar to modern day Florida (Fig. 1B).

Climate at mid-latitudes shifted during the Late Paleocene (Fig. 1C). While northern high latitudes were still relatively cool and wet (CT), mid-latitudes became increasingly dry with arid (WA/CA) to semi-arid conditions (WS/CS) and increasingly intermittent and intense precipitation. Figure 2 depicts the percent of proxy locations that are comprised of each climate type. The proxy locations represent climate at discrete locations and are unevenly distributed throughout the globe, so they should not be considered to be wholly representative of climate. Nonetheless, the percentage of different climate types in each period is useful for discerning temporal changes in climate based on the available data. The number of proxy locations indicative of semi-arid (WS/CS) climates increased from 10–20% compared to the Early Paleocene, and they persisted at about 20–30% of the global climate until the Post-EECO (Fig. 2). Furthermore, proxy locations with WA or CA climates appeared during this time period as far north as ~ 45° latitude in western North America and Europe, indicating precipitation that was much lower annually and more intermittent compared to today. The equator was warm and either monsoonal or ever-wet (WM or WEW). High southern latitudes remained cool with perennial or seasonal precipitation (CT or CM).

The PETM (Fig. 1D) shows an intensification of the trends that began in the Late Paleocene. High northern and southern latitudes were cool with perennial precipitation (CT or CEW). Mid-latitudes became increasingly arid and virtually all perennial climates disappeared from 30–60° latitude. Semi-arid climate (WS/CS) was the most common climate at this time, and arid locations can be observed as far north as 50°, indicating a 5° poleward expansion in the maximum latitude of arid climate (WA/CA) compared to the Late Paleocene. Subtropical latitudes were semi-arid (WS/CS) at ~ 20°N and the equator remained warm and wet (WEW).

Despite a decrease in temperatures and atmospheric carbon dioxide globally, the post-PETM and EECO (Fig. 1E and 1F) climate remained largely unchanged with slightly wetter and less seasonally variable conditions in Western Eurasia compared to the PETM. It was only during the post-EECO cooling (Fig. 1G)

that climate began to once again resemble the modern world, except for the ice-free, wet poles. Despite the sparsity of proxy locations for this time period, it is apparent that mid-latitudes shifted back to a cool, relatively wet climate (CT) while the equator remained similar to today (WEW).

New Insights Into Extremely Warm Climates

Our data illustrate how the Earth system responds to rapidly increasing, high carbon dioxide concentrations, and underline fundamental differences in global climate under such conditions. We also show how Earth system responses vary temporally and latitudinally.

While the lack of polar ice caps and the equitable nature of the extremely warm Early Eocene climates have been previously documented[26, 27], we show that CEW climates already existed at high northern latitudes during the Early Paleocene when carbon dioxide concentrations were only 400 ppm[2], indicating significant shifts in climate already at relatively low carbon dioxide concentrations (Fig. 1B). Monsoonal conditions (CM) were observed on the Antarctic Peninsula during all time periods where proxy data was available. Despite dramatic increases and decreases in atmospheric carbon dioxide concentrations and global temperature through the Paleocene and Early Eocene, polar climate was relatively stable, particularly in the Arctic (Fig. 1).

Another striking change in climate was the drying and increased precipitation intermittency indicated by expansion of arid to semi-arid conditions (WA/CA and WS/CS) at mid-latitudes beginning in the Late Paleocene and persisting until after the EECO (Fig. 2). There are a few data points indicating aridity and intermittent precipitation at about 30° latitude in the Early Paleocene (Fig. 2), but by the Late Paleocene, the most common climate type at mid-latitudes was WS/CS (Fig. 2), indicating a significant increase in aridity and precipitation intermittency at increasingly high latitudes in response to greenhouse gas emissions. A global, mid-latitude increase in precipitation intermittency for the PETM has been noted previously[12, 15], but here we show that these conditions persisted throughout the Early Paleogene. Basin-specific studies have noted dramatic changes in climate prior to and persisting after the PETM[28–30], and this compilation suggests a global significance of these trends. This highlights the scale of potential future changes in precipitation, and the importance of understanding the drivers and timing of shifts in climate variability[31].

As temperatures and atmospheric carbon dioxide concentrations were highest during the PETM, the largest changes in precipitation would also be expected at that time. Much of the prior research has focused on the PETM due to the expectation of dramatic Earth system changes at that time[8, 9, 12]. However, our data are indicative of a significant intensification of the hydrologic cycle that already occurred in the Late Paleocene. Furthermore, precipitation did not significantly change in the post-PETM when mean temperature and atmospheric carbon dioxide concentrations dropped globally (Fig. 1E and Fig. 2)[2]. Based on this global data compilation, the hydrologic cycle did not return to “normal” conditions, similar to the modern day, until the post-EECO cooling period.

Due to the global prevalence of study sites with increased precipitation intermittency and drying persisting after the PETM, our data suggest that spatial shifts in precipitation persist longer than initial carbon dioxide sequestration, especially by the geologically rapid sources such as ocean uptake. Furthermore, based on shifts that occurred specifically during and after the PETM, regions on the border of climate "zones," such as ~ 45° latitude in the western United States and Eurasia, were the most affected by the geologically rapid changes in carbon dioxide emissions, as arid (WA/CA) proxy locations expanded by ~ 5° poleward (Fig. 1 and S2). These findings support interpretations of regionally complex changes in precipitation in high carbon dioxide climates[15].

Implications for Climate Modeling

Our data indicate that boundary conditions suggested for Eocene climate models[32] do not match the proxy record compiled here. For example, vegetation in the Eocene United States is treated as a tropical forest to warm-temperate forest in climate models[32], while this proxy data compilation indicates climate was arid to semi-arid (WA/CA or WS/CS), resulting in the dominance of grasslands and shrubs (Extended data Fig. 2)[29, 34, 35]. Vegetation has a significant impact on climate change through albedo, water vapor production, and cloud formation[36], making its realistic distribution in models essential for understanding climate. Pollen-based reconstructions of vegetation during the PETM[37] indicate warmer, wetter conditions in the United States than the semi-arid conditions indicated by this compilation. This highlights the importance of a multi-proxy approach that considers precipitation intermittency and seasonality in addition to mean conditions, and collaboration between disciplines, to resolve discrepancies.

Cool, ever-wet northern high latitudes and monsoonal southern high latitudes beginning in the Early Paleocene, and increasingly arid, intermittent precipitation at mid-latitudes beginning in the Late Paleocene are indicative of drastic global changes in climate earlier than previously thought[12]. A better understanding of these changes is paramount for understanding and predicting changes resulting from greenhouse gas emissions and sustained warmth. Current models for the warm Early Eocene have indicated increased climate sensitivity as a crucial mechanism for reconstructing pole to equator warmth[38]. However, this does not address other differences in the global distribution of climate compared to today, namely arid and intermittent mid-latitudes and cool monsoonal conditions in Antarctica[39].

Increased aridity and precipitation intermittency at mid-latitudes and other climate changes during the Early Paleogene are indicative of fundamental changes in atmospheric circulation and the hydrological cycle. Possible drivers for these changes are the sustained warmth of the Early Paleogene, changes in the land-sea temperature contrast, a reduced pole to equator temperature gradient, or changes in the outline and height of continents and oceans. The potential hydrological consequences are increases in extreme precipitation from atmospheric rivers and extratropical storms[17], or a poleward shift in the occurrence of tropical cyclones[40]. Today, large population and agricultural centers are located in mid-latitudes[41]. Understanding the mechanisms and potential for droughts and extreme precipitation events in response to warming is paramount to planning for and adapting to climate change.

Declarations

Acknowledgments: We would like to thank the National Science Foundation for funding this work with grant number 2103120. Thank you to Leland Spangler and Maddie Fox for their help with compiling climate data for this study as undergraduate students, and Molly O'Halloran, Patrick Sullivan, and Marion McKenzie for their thoughtful comments on earlier drafts of this work.

Author contributions:

Conceptualization: JSS, PPB

Methodology: JSS, PPB

Investigation: JSS, PPB

Visualization: JSS, PPB, TR, DB

Funding acquisition: PPB, TR

Project administration: JSS, PPB

Supervision: PPB

Writing – original draft: JSS

Writing – review & editing: JSS, PPB, TR, DB

Competing interests: Authors declare that they have no competing interests.

Data and materials availability: All data are available in the main text or the supplementary information.

References

1. K. D. Burke, J. W. Williams, M. A. Chandler, A. M. Haywood, D. J. Lunt, B. L. Otto-Bliesner, Pliocene and Eocene provide best analogs for near-future climates. *Proc. Natl. Acad. Sci. U. S. A.* **115**, 13288–13293 (2018).
2. J. E. Tierney, C. J. Poulsen, I. P. Montañez, T. Bhattacharya, R. Feng, H. L. Ford, B. Hönisch, G. N. Inglis, S. V. Petersen, N. Sagoo, C. R. Tabor, K. Thirumalai, J. Zhu, N. J. Burls, G. L. Foster, Y. Goddéris, B. T. Huber, L. C. Ivany, S. K. Turner, D. J. Lunt, J. C. McElwain, B. J. W. Mills, B. L. Otto-Bliesner, A. Ridgwell, Y. G. Zhang, Past climates inform our future. *Science*. **370** (2020), doi:10.1126/science.aay3701.
3. M. J. Carmichael, G. N. Inglis, M. P. S. Badger, B. D. A. Naafs, L. Behrooz, S. Remmelzwaal, F. M. Monteiro, M. Rohrssen, A. Farnsworth, H. L. Buss, A. J. Dickson, P. J. Valdes, D. J. Lunt, R. D. Pancost,

Hydrological and associated biogeochemical consequences of rapid global warming during the Paleocene-Eocene Thermal Maximum. *Glob. Planet. Change*. **157**, 114–138 (2017).

4. J. C. Zachos, G. R. Dickens, R. E. Zeebe, An early Cenozoic perspective on greenhouse warming and carbon-cycle dynamics. *Nature*. **451**, 279–283 (2008).
5. W. Cornwall, Europe's deadly floods leave scientists stunned. *Science*. **373**, 372–373 (2021).
6. V. Lauretano, J. C. Zachos, L. J. Lourens, Orbitally Paced Carbon and Deep-Sea Temperature Changes at the Peak of the Early Eocene Climatic Optimum. *Paleoceanogr. Paleoclimatology*. **33**, 1050–1065 (2018).
7. Y. Li, P. Sun, Z. Liu, Y. Bai, Y. Xu, L. Ma, R. Liu, Eocene hyperthermal events in the terrestrial system: Geochronological and astrochronological constraints in the Fushun Basin, NE China. *Mar. Pet. Geol.* **139**, 105604–105604 (2022).
8. M. J. Kraus, F. A. McInerney, S. L. Wing, R. Secord, A. A. Baczynski, J. I. Bloch, Paleohydrologic response to continental warming during the Paleocene-Eocene Thermal Maximum, Bighorn Basin, Wyoming. *Palaeogeogr. Palaeoclimatol. Palaeoecol.* **370**, 196–208 (2013).
9. S. L. Wing, G. J. Harrington, F. A. Smith, J. I. Bloch, D. M. Boyer, K. H. Freeman, Transient Floral Change and Rapid Global Warming at the Paleocene-Eocene Boundary. *Science*. **310**, 993–996 (2005).
10. R. E. Zeebe, A. Ridgwell, J. C. Zachos, Anthropogenic carbon release rate unprecedented during the past 66 million years. *Nat. Geosci.* **9**, 325–329 (2016).
11. K. J. Matthews, K. T. Maloney, S. Zahirovic, S. E. Williams, M. Seton, R. D. Müller, Global plate boundary evolution and kinematics since the late Paleozoic. *Glob. Planet. Change*. **146**, 226–250 (2016).
12. F. A. Mcinerney, S. L. Wing, The Paleocene-Eocene Thermal Maximum: A Perturbation of Carbon Cycle, Climate, and Biosphere with Implications for the Future INTRODUCTION AND BRIEF HISTORY OF STUDY. *Annu. Rev. Earth Planet. Sci. Online Earthannualreviewsorg*. **39**, 489–516 (2011).
13. K. Littler, U. Röhl, T. Westerhold, J. C. Zachos, A high-resolution benthic stable-isotope record for the South Atlantic: Implications for orbital-scale changes in Late Paleocene–Early Eocene climate and carbon cycling. *Earth Planet. Sci. Lett.* **401**, 18–30 (2014).
14. C. J. Hollis, T. Dunkley Jones, E. Anagnostou, P. K. Bijl, M. J. Cramwinckel, Y. Cui, G. R. Dickens, K. M. Edgar, Y. Eley, D. Evans, G. L. Foster, J. Frieling, G. N. Inglis, E. M. Kennedy, R. Kozdon, V. Lauretano, C. H. Lear, K. Littler, L. Lourens, A. Nele Meckler, B. D. A. Naafs, H. Pälike, R. D. Pancost, P. N. Pearson, U. Röhl, D. L. Royer, U. Salzmann, B. A. Schubert, H. Seebeck, A. Sluijs, R. P. Speijer, P. Stassen, J. Tierney, A. Tripati, B. Wade, T. Westerhold, C. Witkowski, J. C. Zachos, Y. Ge Zhang, M. Huber, D. J. Lunt, The DeepMIP contribution to PMIP4: Methodologies for selection, compilation and analysis of latest Paleocene and early Eocene climate proxy data, incorporating version 0.1 of the DeepMIP database. *Geosci. Model Dev.* **12**, 3149–3206 (2019).
15. M. J. Carmichael, R. D. Pancost, D. J. Lunt, Changes in the occurrence of extreme precipitation events at the Paleocene–Eocene thermal maximum. *Earth Planet. Sci. Lett.* **501**, 24–36 (2018).

16. I. M. Held, B. J. Soden, Robust Responses of the Hydrological Cycle to Global Warming. *J. Clim.* **19**, 5686–5699 (2006).
17. W. D. Rush, J. T. Kiehl, C. A. Shields, J. C. Zachos, Increased frequency of extreme precipitation events in the North Atlantic during the PETM: Observations and theory. *Palaeogeogr. Palaeoclimatol. Palaeoecol.* **568** (2021), doi:10.1016/j.palaeo.2021.110289.
18. B. A. Schubert, A. H. Jahren, J. J. Eberle, L. S. L. Sternberg, D. A. Eberth, A summertime rainy season in the Arctic forests of the Eocene. *Geology*. **40**, 523–526 (2012).
19. P. A. O'Gorman, Precipitation Extremes Under Climate Change. *Curr. Clim. Change Rep.* **1**, 49–59 (2015).
20. F. Tateo, Clay Minerals at the Paleocene–Eocene Thermal Maximum: Interpretations, Limits, and Perspectives. *Minerals*. **10(12)** (2020).
21. R. H. Whittaker, Classification of natural communities. *Bot. Rev.* **28**, 1–239 (1962).
22. M. C. Peel, B. L. Finlayson, T. A. Mcmahon, "Hydrology and Earth System Sciences Updated world map of the Köppen-Geiger climate classification" (2007), pp. 1633–1644.
23. L. Zhang, C. Wang, X. Li, K. Cao, Y. Song, B. Hu, D. Lu, Q. Wang, X. Du, S. Cao, A new paleoclimate classification for deep time. *Palaeogeogr. Palaeoclimatol. Palaeoecol.* **443**, 98–106 (2016).
24. S. Brönnimann, A. M. Fischer, E. Rozanov, P. Poli, G. P. Compo, P. D. Sardeshmukh, Southward shift of the northern tropical belt from 1945 to 1980. *Nat. Geosci.* **8**, 969–974 (2015).
25. B. Wang, Q. Ding, Global monsoon: Dominant mode of annual variation in the tropics. *Dyn. Atmospheres Oceans*. **44**, 165–183 (2008).
26. J. Zachos, M. Pagani, L. Sloan, E. Thomas, K. Billups, Trends, Rhythms, and Aberrations in Global Climate 65 Ma to Present. *Science*. **292**, 686–693 (2001).
27. M. J. Cramwinckel, M. Huber, I. J. Kocken, C. Agnini, P. K. Bijl, S. M. Bohaty, J. Frieling, A. Goldner, F. J. Hilgen, E. L. Kip, F. Peterse, R. Van Der Ploeg, U. Röhl, S. Schouten, A. Sluijs, Synchronous tropical and polar temperature evolution in the Eocene. *Nature*. **559**, 382–386 (2018).
28. P. Xue, L. Chang, E. Thomas, Abrupt Northwest Atlantic deep-sea oxygenation decline preceded the Palaeocene-Eocene Thermal Maximum. *Earth Planet. Sci. Lett.* **618**, 118304–118304 (2023).
29. K. L. Zellman, P. Plink-Björklund, H. C. Fricke, Testing hypotheses on signatures of precipitation variability in the river and floodplain deposits of the paleogene san juan basin, New Mexico, U.S.A. *J. Sediment. Res.* **90**, 1770–1801 (2020).
30. B. Z. Foreman, P. L. Heller, M. T. Clementz, Fluvial response to abrupt global warming at the Palaeocene/Eocene boundary. *Nature*. **491**, 92–95 (2012).
31. A. J. McMichael, R. E. Woodruff, S. Hales, Climate change and human health: present and future risks. *The Lancet*. **367**, 859–869 (2006).
32. R. Knutti, J. Sedláček, Robustness and uncertainties in the new CMIP5 climate model projections. *Nat. Clim. Change*. **3**, 369–373 (2013).

33. N. Herold, J. Buzan, M. Seton, A. Goldner, J. A. M. Green, R. D. Müller, P. Markwick, M. Huber, A suite of early Eocene (~ 55 Ma) climate model boundary conditions. *Geosci. Model Dev.* **7**, 2077–2090 (2014).
34. L. P. Birgenheier, M. D. V. Berg, P. Plink-Björklund, R. D. Gall, E. Rosencrans, M. J. Rosenberg, L. C. Toms, J. Morris, Climate impact on fluvial-lake system evolution, Eocene Green River Formation, Uinta Basin, Utah, USA. *Bull. Geol. Soc. Am.* **132**, 562–587 (2020).
35. E. I. Woodward, B. G. Williams, "Climate and plant distribution at global and local scales" (1987), pp. 189–197.
36. C. A. Loptson, D. J. Lunt, J. E. Francis, Investigating vegetation–climate feedbacks during the early Eocene. *Clim. Past*. **10**, 419–436 (2014).
37. V. A. Korasidis, S. L. Wing, C. A. Shields, J. T. Kiehl, Global Changes in Terrestrial Vegetation and Continental Climate During the Paleocene-Eocene Thermal Maximum. *Paleoceanogr. Paleoclimatology*. **37** (2022), doi:10.1029/2021PA004325.
38. J. Zhu, C. J. Poulsen, J. E. Tierney, Simulation of Eocene extreme warmth and high climate sensitivity through cloud feedbacks. *Sci. Adv.* **5**, eaax1874 (2019).
39. M. Baatsen, P. Bijl, A. Von Der Heydt, A. Sluijs, H. Dijkstra, Resilient Antarctic monsoonal climate prevented ice growth during the Eocene, doi:10.5194/cp-2023-36.
40. J. T. Kiehl, C. M. Zarzycki, C. A. Shields, M. V. Rothstein, Simulated changes to tropical cyclones across the Paleocene-Eocene Thermal Maximum (PETM) boundary. *Palaeogeography, Palaeoclimatology, Palaeoecology*. **572**, 110421 (2021).
41. D. B. Lobell, W. Schlenker, J. Costa-Roberts, Climate Trends and Global Crop Production Since 1980. *Science*. **333**, 616–620 (2011).

Methods

We collected all of the available climate data for the Early Paleocene through the EECO (66-49 Ma) from literature published in peer review articles. Information extracted included MAT, MAP, precipitation intermittency, and proxy type. Where only qualitative data was available, a range of MAT, MAP, and precipitation intermittency were estimated based on the proxy information (see SI "Climate type definitions").

Based on the Köppen-Geiger system[22], Whittaker vegetation plots[21], and the available climate data, we designed a comprehensive system for describing Early Paleogene climate type with a focus on mean annual precipitation and precipitation intermittency (Table 1 and SI "Climate type definitions"). Climate types are defined based on MAT, MAP, and precipitation intermittency. The Köppen-Geiger system was not used because it requires information that is not discernible in the geologic record, and it does not address the intermittency of precipitation, which is essential to understanding an environment. The paleo-Köppen-Geiger system from Zhang et al. (2016) was also not utilized because it does not address precipitation intermittency.

With clearly defined climate types and the global data compilation completed, each proxy location was assigned a climate type and associated uncertainty value from 1-5, where 5 is the most uncertain (Extended data Fig. 1). Uncertainty was assigned based on the quantitative or qualitative error associated with each proxy[3, 14], and high uncertainty values were assigned when proxy uncertainty could lead to the assignment of a different climate type. Where multiple proxies contained similar information for a study site, uncertainty was considered to be very low (1). To view the MAP, MAT, precipitation intermittency, and uncertainty value for each site, view the site spreadsheet (SI Data S1) or interactive maps (SI Data S2 or S3).

The maps were built using Matthews et al. (2016) plate model in gplates v.2.3 (https://www.gplates.org/). Individual shapefiles of the sites at their modern locations for each time period were made using QGIS v.3.28 (https://www.qgis.org/en/site/index.html), then the shapefiles were projected onto the gplates reconstruction at a time of 0 Ma. The site points were tied to the tectonic plates at their modern location then moved back in time to their respective time period. Shapefiles for the Early Paleocene, Late Paleocene, PETM, Post-PETM, EECO, and Post-EECO were then extracted from gplates back into GIS software with sites at their correct paleolatitude and paleolongitude. Because these time periods took place over millions of years, a single time had to be chosen as representative of each time period.

Figures

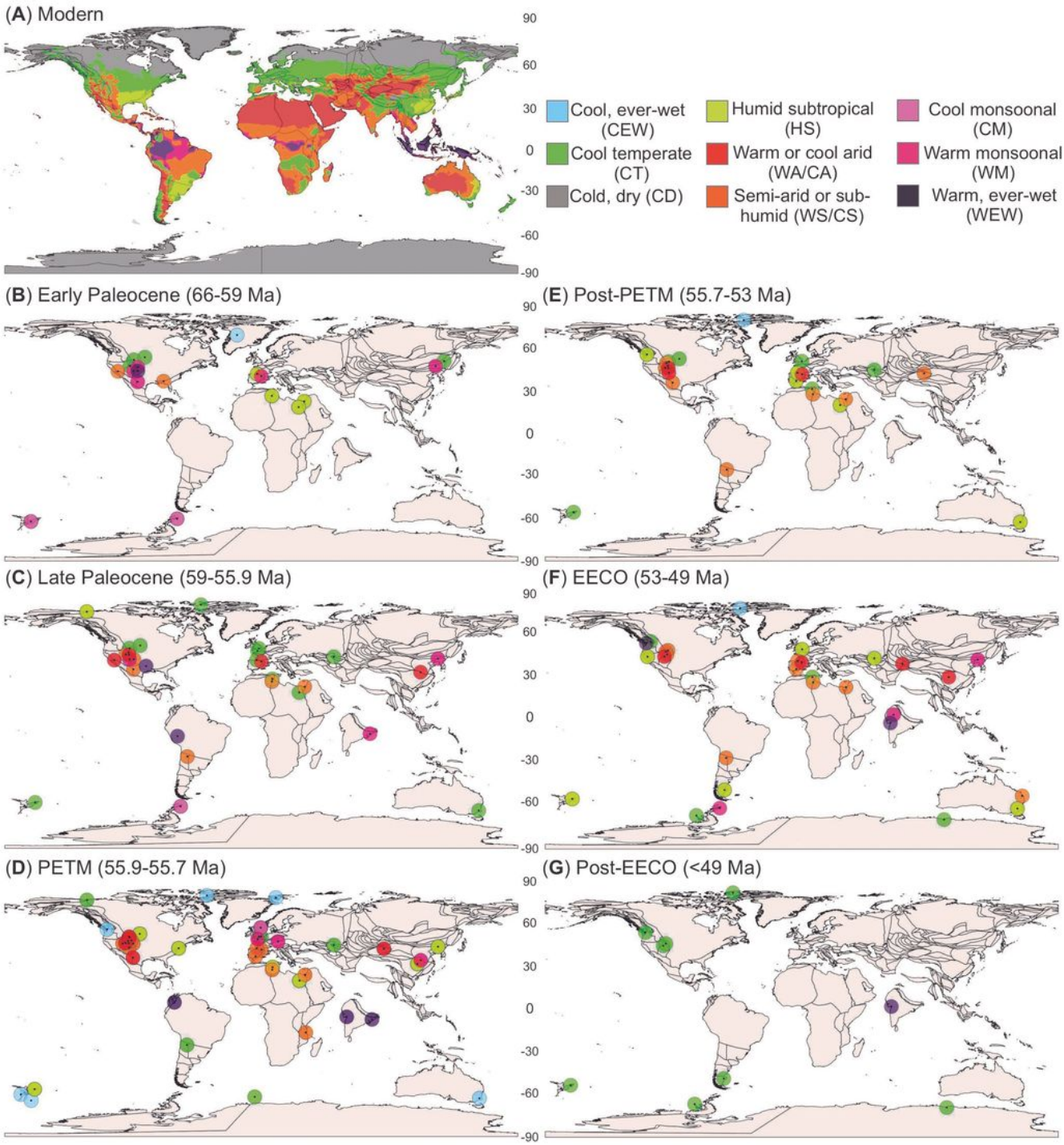

Figure 1

Climate in the modern world (A) and Early Paleogene (B-G). The Early Paleogene point data correspond to proxy locations. The modern climate type distribution was adapted from Peel et al., 2007 *(22)*. Note the increase in arid and semi-arid conditions (WA/CA and WS/CS) in mid-latitudes beginning in the Late Paleocene.

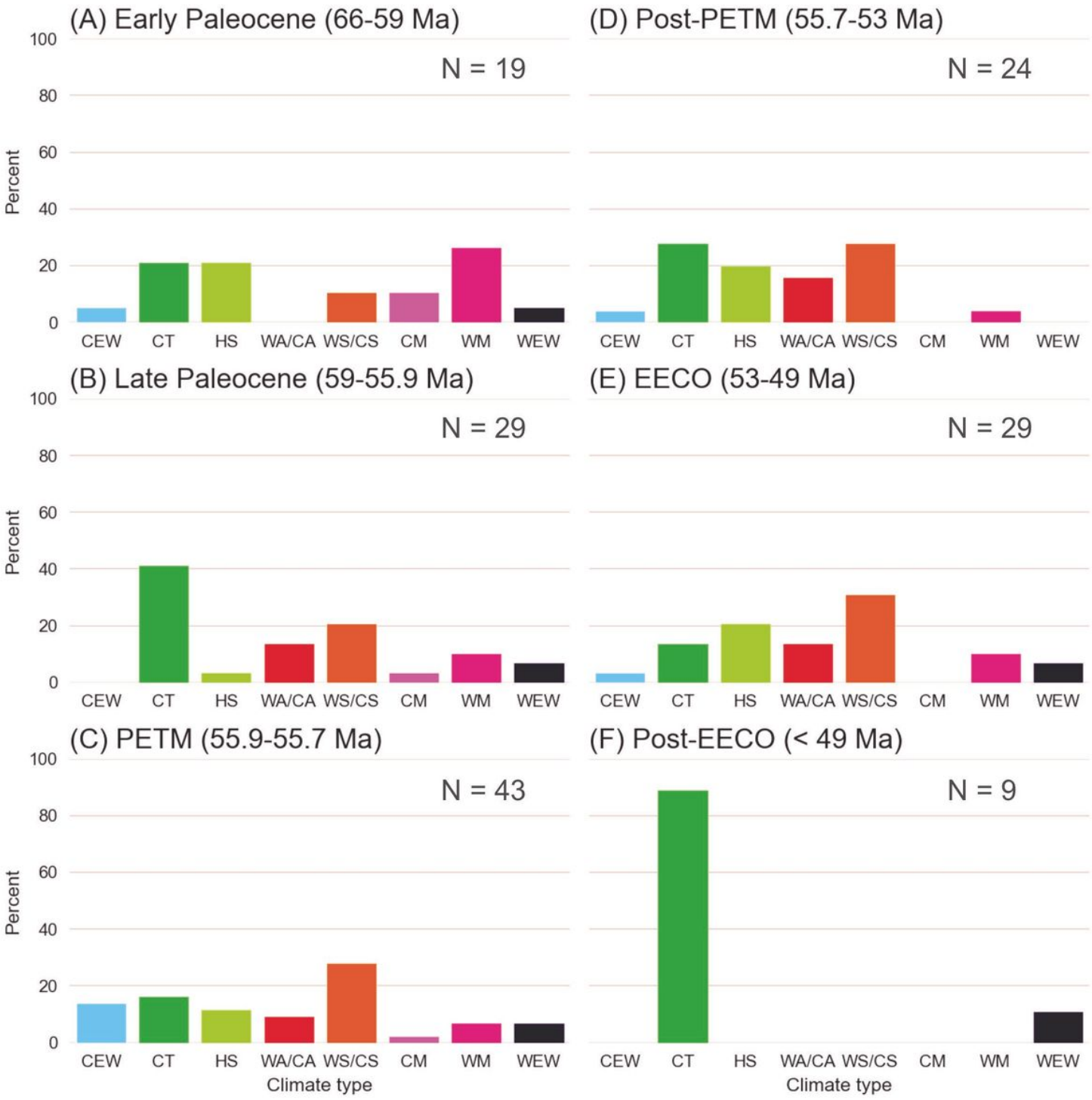

Figure 2

Relative frequency histograms showing the number of observations of each climate type through the Early Paleogene. The relative frequency histograms highlight the increase in WS/CS and WA/CA beginning in the Late Paleocene and persisting until after the EECO. Note that there are far fewer proxy locations in the post-EECO. The acronyms correspond to the climate types described in Table 1.

Supplementary Files

This is a list of supplementary files associated with this preprint. Click to download.

- NatureSupplementaryMaterials.docx
- Extendeddata.docx